

QUASI-SEPARATRIX LAYERS: REFINED THEORY AND ITS APPLICATION TO SOLAR FLARES

V.S. Titov¹, P. Démoulin² and G. Hornig¹

¹Theoretische Physik IV, Ruhr-Universität Bochum, 44780 Bochum, Germany

²DASOP, Observatoire de Paris-Meudon, F 92195 Meudon cedex, France

ABSTRACT

Although the analysis of observational data indicates that quasi-separatrix layers (QSLs) have to play an important role in magnetic configurations of solar flares, the corresponding theory is only at an initial stage so far. In particular, there is still a need in a proper definition of QSL. This problem is analyzed here on the basis of geometrical properties of the mapping produced by the field lines which connect photospheric areas of positive and negative magnetic polarities of active regions. In general, one can find on the photosphere a unique pair of locally perpendicular line elements at one footpoint of a given field line, so that this pair is mapped into a similar pair of elements at the other footpoint. Along the directions of these elements the field line mapping only stretches and compresses the corresponding displacements of the neighboring field-line footpoints. This fact enables us to get a remarkably clear and concise definition of QSL as a volume filled by coronal field lines for which the ratio of the corresponding stretching and compressing coefficients is anomalously large. The new definition is also compared with the ones previously introduced by other authors.

The theory is applied to flare events of the so-called sigmoid-type, using an analytical model of a twisted force-free configuration (Titov & Démoulin 1999a, b). It is shown that such a configuration may contain a QSL even if genuine separatrix surfaces are absent. Identifying QSLs is an essential prerequisite for understanding the mechanism of magnetic energy release in this type of flares. It is also demonstrated that the magnetic field under study has a Hamiltonian structure, which makes it possible to reveal a geometrical reason for the appearance of QSL in this case.

Key words: Quasi-separatrix layers; magnetic topology; solar flares.

ways show a relation of solar flares with the separatrices caused by magnetic null points (Démoulin et al. 1994). There is, however, a more systematic spatial correlation between the locations of energy release in flares and the regions of strong variation of the field line connectivity (e.g. Mandrini et al. 1995, Démoulin et al. 1997). Such regions, called quasi-separatrix layers (QSLs), are thought to be the plausible places for the magnetic reconnection process (Priest & Démoulin 1995).

In most of the coronal volume the quasi-static conditions are fulfilled, so that the magnetic field evolves through a sequence of force-free equilibria. These conditions, however, may easily break down in QSLs, where due to a strong variation of the field line connectivity the rearrangement of the field lines during the evolution of the configuration may occur faster than in other places. This in turn implies a locally large acceleration of plasma and hence a locally unbalanced and enhanced Lorentz force with corresponding concentrations of the current density. So ultimately the inertia of plasma may cause the formation of current layers in QSLs. The importance of inertia in the current layers at the QSLs is also followed from exact solutions of linearized MHD equations describing a quasi-static evolution of inhomogeneous magnetic fields (Invernarity & Titov 1997).

The paper is organized as follows. In Sec. 2, we discuss the difference between separatrix surfaces and QSLs together with the primary definition of QSLs. In Sec. 3, the local geometrical properties of the magnetic connectivity are studied. The new geometrical measure for QSLs is derived and compared with the old ones. Sec. 4 contains an application of this theory to a model of flaring twisted configurations possessing a Hamiltonian structure, which plays an important role in the formation of QSLs. The conclusions are summarized in Sec. 5.

2. THE QSL AND ITS PRIMARY DEFINITION

The magnetic field lines in solar active regions normally connect domains of positive and negative polarity of the photospheric plane, say, $z = 0$. Let the location of their footpoints in this plane be represented depending on the polarity by the radius-vector $\mathbf{r}_+ = (x_+, y_+)$ or $\mathbf{r}_- = (x_-, y_-)$. The con-

1. INTRODUCTION

Investigations of coronal magnetic fields extrapolated from photospheric magnetograms do not al-

nections of the footpoints by the field lines determine two mutually inverse mappings $\Pi_- : \mathbf{r}_+ \mapsto \mathbf{r}_-$ and $\Pi_+ : \mathbf{r}_- \mapsto \mathbf{r}_+$. We shall simply use Π if we refer to aspects valid for both mappings. Also the functional forms $(X_-(\mathbf{r}_+), Y_-(\mathbf{r}_+)) \equiv \Pi_-(\mathbf{r}_+)$ and $(X_+(\mathbf{r}_-), Y_+(\mathbf{r}_-)) \equiv \Pi_+(\mathbf{r}_-)$ will be used further for the mappings.

The mapping Π is discontinuous at the footpoints of the field lines threading magnetic nulls in the corona or touching the photosphere, since the magnetic flux tubes enclosing such field lines are splitted at the nulls or at the touching points (Seehafer 1986). The corresponding discontinuities serve as indicators for the separatrix field lines and surfaces. It is worth to emphasize that the coordinates (x_{\pm}, y_{\pm}) in this case need not to be Cartesian because the discontinuities are revealed in any system of coordinates irrespective of the metrics.

However, with the help of the metrics or Cartesian coordinates one can determine not only the genuine separatrices but also the QSLs. The integrity of the flux tubes is preserved within the QSLs and so the mapping Π remains continuous at the corresponding footpoints, but the shape of their cross-sections strongly change along the flux tubes. Thus, instead of the true discontinuities in Π at the intersection of the genuine separatrices with the photosphere, there are continuous but rapid variations in Π at the photospheric cross-sections of QSLs. These variations can only be detected by using the metrics, which enables us to measure and compare the distances between the footpoints in one polarity and corresponding footpoints in the other polarity. In this respect QSLs and separatrices are qualitatively different objects. Indeed, ignoring the above metrical information about Π and using a proper continuous change of coordinates, it is possible to eliminate the rapid variations in Π and thereby the QSLs themselves, while the discontinuities of Π and hence the corresponding separatrices are not removable in this way. However, for physical processes with characteristic length scales much less than the QSL thickness such a QSL must be as important as a genuine separatrix.

For the determination of the QSLs Priest & Démoulin (1995) proposed to use the function (called “the norm”) $N(\mathbf{r}_+)$ or $N(\mathbf{r}_-)$, which in Cartesian coordinates are

$$N(\mathbf{r}_{\pm}) = \left[\left(\frac{\partial X_{\mp}}{\partial x_{\pm}} \right)^2 + \left(\frac{\partial X_{\mp}}{\partial y_{\pm}} \right)^2 + \left(\frac{\partial Y_{\mp}}{\partial x_{\pm}} \right)^2 + \left(\frac{\partial Y_{\mp}}{\partial y_{\pm}} \right)^2 \right]^{1/2} \equiv N_{\pm}. \quad (1)$$

It was suggested that $N(\mathbf{r}_{\pm}) \gg 1$ at the footpoints of the field lines belonging to QSLs and $N(\mathbf{r}_{\pm}) \approx 1$ otherwise. Yet this norm in application to different footpoints of the same field line yields generally different values N_+ and N_- , which leads to an ambiguity in the determination of QSLs. This disadvantage of the norm indicates that the adequate measure for QSLs must be invariant to the choice of the mapping Π_- or Π_+ . Below we find such a measure by analyzing geometrical properties of the field line connectivity.

3. REVISED DEFINITION OF QSL

The mapping Π_- or Π_+ is locally described by its differential Π_-^* or Π_+^* , respectively, which is a linear mapping from the plane tangent to the photosphere at one footpoint to a similar plane at the other footpoint. These differentials are represented by the corresponding, mutually inverse, Jacobian matrices

$$\mathcal{D} = \begin{pmatrix} \frac{\partial X_-}{\partial x_+} & \frac{\partial X_-}{\partial y_+} \\ \frac{\partial Y_-}{\partial x_+} & \frac{\partial Y_-}{\partial y_+} \end{pmatrix} \equiv \begin{pmatrix} a & b \\ c & d \end{pmatrix} \quad (2)$$

and

$$\mathcal{D}_+ = \begin{pmatrix} \frac{\partial X_+}{\partial x_-} & \frac{\partial X_+}{\partial y_-} \\ \frac{\partial Y_+}{\partial x_-} & \frac{\partial Y_+}{\partial y_-} \end{pmatrix} = \Delta_+^{-1} \begin{pmatrix} d & -b \\ -c & a \end{pmatrix}, \quad (3)$$

$$\Delta_+ = ad - bc \equiv \det \mathcal{D}. \quad (4)$$

We assume hereafter that (x_{\pm}, y_{\pm}) are measured in one Cartesian system of coordinates covering the whole photospheric plane. Eqs. (2) and (3) show that it is sufficient to have only one of these matrices for a local description of the magnetic connectivity.

An orthonormal vector basis $(\hat{\mathbf{u}}_+, \hat{\mathbf{v}}_+)$ in the tangent plane at some footpoint \mathbf{r}_+ is generally mapped by Π_-^* into a non-orthonormal basis $(\mathbf{u}_-, \mathbf{v}_-)$ with $\mathbf{u}_- = \mathcal{D} \hat{\mathbf{u}}_+$ and $\mathbf{v}_- = \mathcal{D} \hat{\mathbf{v}}_+$ in the corresponding tangent plane at $\Pi_-(\mathbf{r}_+)$ (Figure 1a). One can choose, however, a special orientation of $(\hat{\mathbf{u}}_+, \hat{\mathbf{v}}_+)$ such that the basis $(\mathbf{u}_-, \mathbf{v}_-)$ becomes orthogonal (Figure 1b). Indeed, let the angles γ_+ and γ_- , respectively, determine the directions of $\hat{\mathbf{u}}_+$ and \mathbf{u}_- with respect to the x -axis of the global Cartesian system of coordinates. \mathcal{R}_{γ_+} and \mathcal{R}_{γ_-} are the corresponding matrices of rotations. It follows then from Figure 1b that $|\mathbf{u}_-| \mathcal{R}_{\gamma_+}^{-1} \hat{\mathbf{u}}_+ = \mathcal{R}_{\gamma_-}^{-1} \mathcal{D} \hat{\mathbf{u}}_+$ and $|\mathbf{v}_-| \mathcal{R}_{\gamma_-}^{-1} \hat{\mathbf{v}}_+ = \mathcal{R}_{\gamma_+}^{-1} \mathcal{D} \hat{\mathbf{v}}_+$ or, in other words,

$$\text{diag}(|\mathbf{u}_-|, |\mathbf{v}_-|) = \mathcal{R}_{\gamma_-}^{-1} \mathcal{D} \mathcal{R}_{\gamma_+}. \quad (5)$$

It means that the two non-diagonal elements at the right hand side of (5) must vanish. This condition can be satisfied by

$$\gamma_+ - \gamma_- = \arg \xi, \quad (6)$$

$$\gamma_+ + \gamma_- = \arg \zeta, \quad (7)$$

where the function \arg determines the arguments of the complex values ($i = \sqrt{-1}$)

$$\xi = a + d + i(b - c), \quad (8)$$

$$\zeta = a - d + i(b + c). \quad (9)$$

This solution for γ_+ and γ_- can be checked by substitution of (2) and the corresponding expressions for the rotation matrices in (5). Other solutions are also possible but not of interest, since they are simply the result of mirror reflections about the directions given by (6) and (7).

Eqs. (5)–(9) and (2) yield

$$|\mathbf{u}_-| = (|\xi| + |\zeta|)/2, \quad (10)$$

$$|\mathbf{v}_-| = (|\xi| - |\zeta|)/2, \quad (11)$$

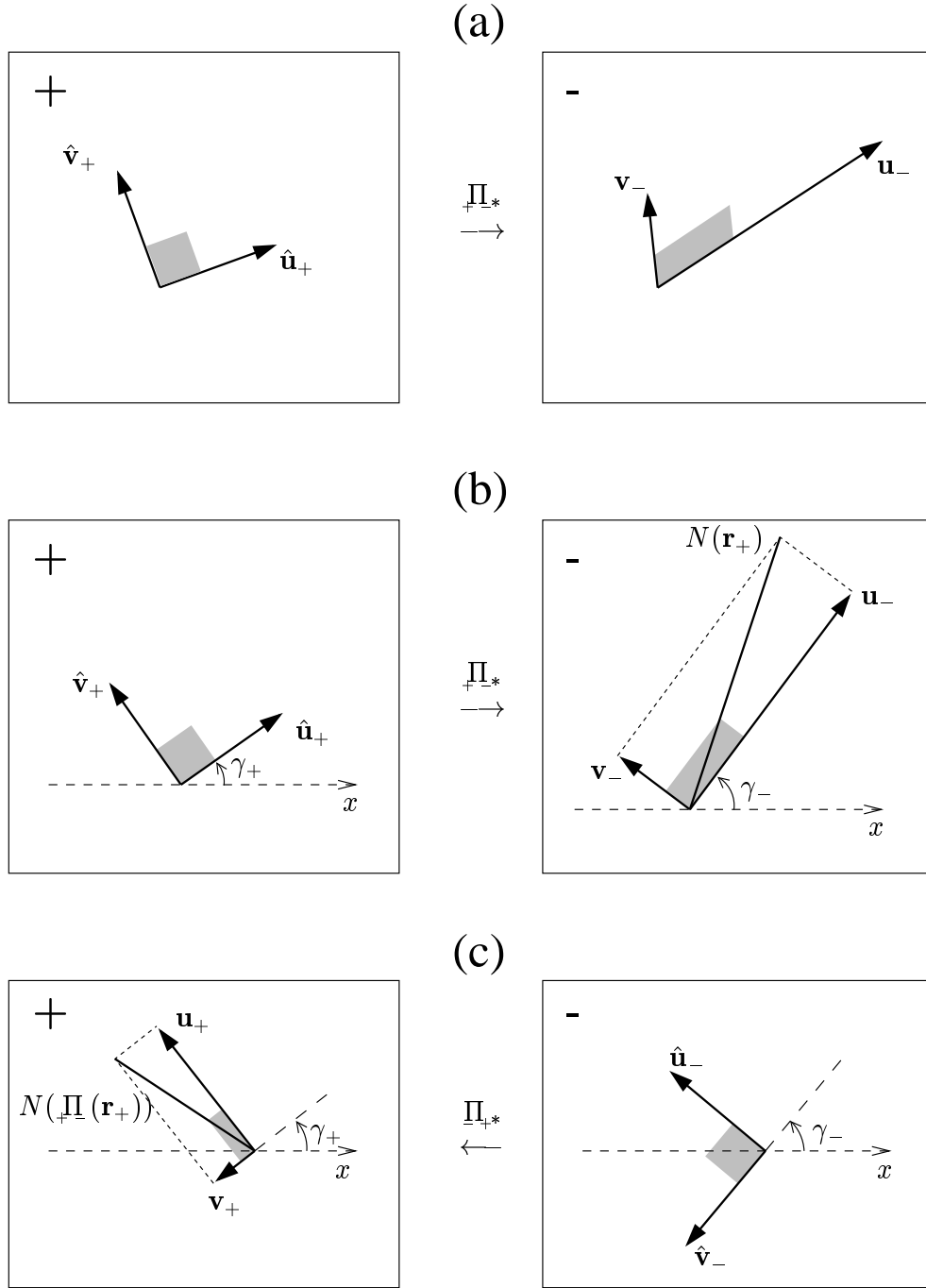


Figure 1. The mapping of an orthonormal basis $(\hat{\mathbf{u}}_+, \hat{\mathbf{v}}_+)$ by the differential Π_{+*} (a,b): its image basis $(\mathbf{u}_-, \mathbf{v}_-)$ is in general non-orthonormal (a), but it is orthogonal for a special orientation of $(\hat{\mathbf{u}}_+, \hat{\mathbf{v}}_+)$ (b) when $|\mathbf{u}_- + \mathbf{v}_-|$ determines the norm $N(\mathbf{r}_+)$. The inverse differential Π_{+*} maps the orthonormal basis $(\hat{\mathbf{u}}_-, \hat{\mathbf{v}}_-)$, rotated with respect to $(\mathbf{u}_-, \mathbf{v}_-)$ on $\pi/2$, into the orthogonal basis $(\mathbf{u}_+, \mathbf{v}_+)$ (c), so that $|\mathbf{u}_+|/|\mathbf{v}_+| = |\mathbf{u}_-|/|\mathbf{v}_-|$ but $|\mathbf{u}_+ + \mathbf{v}_+| = N(\Pi_+(\mathbf{r}_+)) \neq N(\mathbf{r}_+)$. The shaded areas show how these properties of the mappings manifest in the corresponding cross-sections of thin flux tubes.

which means that $|\mathbf{u}_-| \geq |\mathbf{v}_-|$ in the solution under consideration. By using these expressions and (1)–(2) one can obtain

$$|\mathbf{u}_- + \mathbf{v}_-| = (a^2 + b^2 + c^2 + d^2)^{1/2} \equiv N_+. \quad (12)$$

Thus the norm N_+ determines simply the length of the rectangular diagonal constructed on the vectors \mathbf{u}_- and \mathbf{v}_- (Figure 1b).

It is worth to determine similar characteristics for

the reverse differential Π_{+*} at $\mathbf{r}_- = \Pi_+(\mathbf{r}_+)$. The simplest way to do this is just to change in (6)–(11) the superscripts \pm on \mp and the elements of \mathcal{D}_- (2) to the corresponding elements of \mathcal{D}_+ (3). Then we obtain for the complex values similar to (8) and (9)

$$\tilde{\xi} = [d + a - i(b - c)]/\Delta_+ \equiv \bar{\xi}/\Delta_+, \quad (13)$$

$$\tilde{\zeta} = [d - a - i(b + c)]/\Delta_+ \equiv -\zeta/\Delta_+, \quad (14)$$

yielding the following equations for the angles:

$$\tilde{\gamma}_- - \tilde{\gamma}_+ = \arg \bar{\xi} \equiv -\arg \xi, \quad (15)$$

$$\tilde{\gamma}_- + \tilde{\gamma}_+ = \arg \zeta + \pi. \quad (16)$$

They show that the orthonormal basis $(\hat{\mathbf{u}}_-, \hat{\mathbf{v}}_-)$ corresponding to this solution is turned on $\pi/2$ with respect to the basis $(\mathbf{u}_-, \mathbf{v}_-)$ and the same is valid for $(\mathbf{u}_+, \mathbf{v}_+)$ and $(\hat{\mathbf{u}}_+, \hat{\mathbf{v}}_+)$ (Figure 1b, c). In application to (10) and (11) the considered transformation gives

$$|\mathbf{u}_+| = 1/|\mathbf{v}_-|, \quad (17)$$

$$|\mathbf{v}_+| = 1/|\mathbf{u}_-|. \quad (18)$$

So the norm in the negative polarity at the footpoint $\mathbf{r}_- = {}_{\perp}\Pi(\mathbf{r}_+)$ is

$$N_- \circ {}_{\perp}\Pi = N_+/|\Delta_+|. \quad (19)$$

This consideration shows that the determination of QSLs by means of the norms N_+ and N_- must really lead to different results if $|\Delta_+| \neq 1$. Combining of these results in order to find the “proper” QSL is in fact equivalent to finding only in the positive polarity the regions where the functions N_+ and $N_+/|\Delta_+|$ acquire anomalously large values. Yet the simultaneous using of two different functions for characterizing QSLs does not look as a theoretically well-founded approach.

One can resolve this difficulty by noticing, first, that the mapping Π can locally be described by $|\mathbf{u}_-|$, $|\mathbf{v}_-|$, γ_+ and γ_- , where only $|\mathbf{u}_-|$ and $|\mathbf{v}_-|$ determine the value of footpoint displacements, while γ_+ and γ_- define their directions. So it would be natural if the required characteristics is a function of $|\mathbf{u}_-|$ and $|\mathbf{v}_-|$ only. We think that the ratio $|\mathbf{u}_-|/|\mathbf{v}_-| \geq 1$ is a more suitable quantity for describing QSLs than the considered above norm. According to (17) and (18) (see also Figure 1b, c) it coincides with the ratio $|\mathbf{u}_+|/|\mathbf{v}_+|$ and thereby characterizes the magnetic connectivity itself rather than one of the mappings ${}_{\perp}\Pi$ or Π_+ . It determines the degree of flattening of the elementary flux tubes at their photospheric ends (see shaded regions in Figure 1b,c), so the tubes characterized by extremely high values of this quantity should be referred to as QSL. By using (8)–(11) one can derive that

$$|\mathbf{u}_-|/|\mathbf{v}_-| = Q/2 + \sqrt{Q^2/4 - 1}, \quad (20)$$

$$Q = N_+^2/|\Delta_+|, \quad (21)$$

which shows that $|\mathbf{u}_-|/|\mathbf{v}_-| \approx Q$ for $Q \gg 1$. It is seen from (19) and (21) that Q is simply a product of the norms N_+ and N_- calculated at the opposite ends of the field lines. Geometrically, the value Q is the ratio of the square of quadrat with the side N_+ to the square of the rectangular based on the vectors \mathbf{u}_- and \mathbf{v}_- , because $|\Delta_+| = |\mathbf{u}_-| \cdot |\mathbf{v}_-|$. Note also that $Q \geq 2$, since N_+ is the length of the diagonal in this rectangular. The expression for Q has an elegant form, invariant to the change $+$ \leftrightarrow $-$ and simpler than (20), so it is reasonable to define:

The QSL is a flux tube consisting of magnetic field lines with $Q \gg 1$.

One can see from (21) that if the determinant Δ_+ varies in the photospheric plane as strong as N_+ , the QSLs defined with the help of Q or N_+ have to be

different, otherwise they must be approximately the same.

Some comments should also be added on another characteristics for determining QSLs, namely, on the so-called differential flux volume

$$V(\mathbf{r}_+) = \int_{\mathbf{r}_+}^{\Pi(\mathbf{r}_+)} \frac{dl}{B} \equiv V({}_{\perp}\Pi(\mathbf{r}_+)),$$

in which the integration is carried out along the corresponding field line. This value has appeared in the analysis of current sheet formations along separatrix surfaces in quasi-static evolutions of $2\frac{1}{2}$ D magnetic configurations (Zwingmann et al. 1985, Low & Wolfson 1988, Vekstein et al. 1991, Vekstein & Priest 1992). It has also been used (under the name “delay function”) for studying 3D magnetic topology caused by the presence of null points (Lau 1993). Recently Schindler & Birn (1999) have shown that strong spatial variations of V may cause a similar formation of current layers in 3D magnetic fields. So it seems natural at first sight to use this value for characterizing QSLs. However, if one fixes the footpoints of the magnetic field lines in a given configuration and exposes the coronal volume to a smooth deformation, then V will be changed depending on such a deformation, while the field line connectivity will remain the same. Thus, the quantity Q as a measure of the field line connectivity is better than V , although this does not reduce the value of V in understanding of the above mentioned current sheet formation.

4. HAMILTONIAN STRUCTURE AND QSL IN FLARING TWISTED CONFIGURATIONS

The topology of a twisted magnetic configuration provides important clues for understanding sigmoid-like flares (Titov & Démoulin 1999a, b). Such a configuration can be modeled by a force-free circular flux tube with total current I , which is embedded into potential field produced by a pair of magnetic charges q , $-q$ and a line current I_0 (Figure 2). The charges are on a distance $2L$ from each other and lie together with the current I_0 on the axis of symmetry of the configuration, which is on the depth d below the photospheric plane $z = 0$. Below this plane the sources and their fields have no a real physical meaning: they are used only to construct the proper magnetic field in the corona. The photospheric vertical component of this field and current density of the flux tube can be considered a posteriori as the corresponding boundary conditions for the resulting configuration.

The construction of this magnetic field excludes the existence of any null point in our model, so the topology of the coronal field may be non-trivial only due to the presence of the so-called bald patches (BPs, see Titov et al. 1993), which are the segments of the photospheric inversion line (IL) where the coronal field lines touch the photosphere (Seehafer 1986). Thus, the separatrices, if present, consist of only the field lines starting at the BPs. The full topological analysis of the field then reduces to determining the BPs and their associated separatrices. Such an analysis has been made by Titov & Démoulin (1999) for the

scenario in which the major radius R of the flux tube (Figure 2) grows, starting from $R = d$, while the intensity and positions of sub-photospheric sources remain constant. It was found that the BP appears first at some $R = R_a > d$ and then grows in size with increasing R . After reaching some $R = R_b > R_a$ the BP bifurcates at the center of the configuration to give birth to a generalized separator field line at the intersection of two separatrix surfaces. The gap between bifurcated parts of BP grows with R , while these parts shrink and eventually disappear at some $R = R_d (> R_b)$, where a transition to a topologically simple arcade-like configuration occurs.

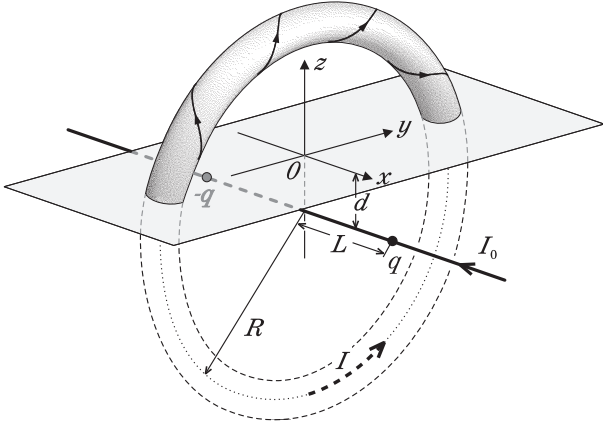


Figure 2. The scheme of the model for the twisted magnetic configuration

In spite of this simplicity, the resulting magnetic field might have QSLs, which are as important as the genuine separatrices under the appropriate conditions. The aim of the further consideration is to check this possibility by using the above theory of QSLs for the same scenario of the magnetic field evolution.

Here we use the cylindrical system of coordinates (r_\perp, θ, x) , whose axis is directed along I_0 and where $r_\perp \equiv |\mathbf{r}_\perp|$ with $\mathbf{r}_\perp \equiv (0, y, z + d)$, θ is the angle between \mathbf{r}_\perp and $\hat{\mathbf{y}}$, and $\hat{\boldsymbol{\theta}}$ is the corresponding unit vector. Due to the axial symmetry about the line current I_0 (Figure 2) the magnetic field can be written as

$$\mathbf{B} = \nabla \times \left(\frac{\Psi}{r_\perp} \hat{\boldsymbol{\theta}} \right) + B_\theta \hat{\boldsymbol{\theta}}, \quad (22)$$

which, in particular, gives

$$B_x = \frac{1}{r_\perp} \frac{\partial \Psi}{\partial r_\perp}. \quad (23)$$

It is convenient in our case to use θ for parameterizing field lines, so that their equation $\mathbf{dr} \times \mathbf{B} = 0$ with $\mathbf{dr} = dr_\perp \hat{\mathbf{r}}_\perp + r_\perp d\theta \hat{\boldsymbol{\theta}} + dx \hat{\mathbf{x}}$ yield

$$\frac{dx}{d\theta} = \frac{1}{B_\theta} \frac{\partial \Psi}{\partial r_\perp}, \quad (24)$$

$$\frac{dr_\perp}{d\theta} = -\frac{1}{B_\theta} \frac{\partial \Psi}{\partial x}. \quad (25)$$

These are the components of the field line equation along $\hat{\mathbf{r}}_\perp$ and $\hat{\mathbf{x}}$, respectively, while the component

along $\hat{\boldsymbol{\theta}}$ requires $d\Psi = 0$ along the field lines, which is simply a consequence of (24)–(25).

The axial symmetry allows also to write the x -component of the current density \mathbf{j} as

$$j_x = \frac{1}{\mu_0 r_\perp} \frac{\partial}{\partial r_\perp} (r_\perp B_\theta),$$

from where after introducing the whole current $J = \int_0^{r_\perp} j_x 2\pi r_\perp dr_\perp$ through the perpendicular to the x -axis disc of radius r_\perp one can obtain

$$B_\theta = \frac{\mu_0 J(\Psi)}{2\pi r_\perp}. \quad (26)$$

Here we put $J = J(\Psi)$, since the current lines lie on magnetic surfaces $\Psi = \text{const}$ (note that in our model $\mathbf{j} \parallel \mathbf{B}$ and $\mathbf{B} \cdot \nabla \Psi = 0$ according to Eq. (22)). Moreover, this is also valid in more general case of magnetostatic configurations. By using (26) and normalizing the coordinates as $\tilde{r}_\perp = r_\perp/L$, $\tilde{x} = x/L$ with subsequent omitting of the tilde, one can transform (24)–(25) to the following one-dimensional and autonomous Hamiltonian system:

$$\frac{dx}{d\theta} = \frac{\partial H}{\partial \varpi}, \quad (27)$$

$$\frac{d\varpi}{d\theta} = -\frac{\partial H}{\partial x}, \quad (28)$$

where θ is a time-like variable and instead of r_\perp the new momentum-like variable

$$\varpi = \ln r_\perp \quad (29)$$

is introduced together with the Hamiltonian function

$$H = \frac{2\pi}{\mu_0 L} \int \frac{d\Psi}{J(\Psi)}. \quad (30)$$

The Hamiltonian structure is revealed here only with the help of the axial symmetry and the magnetostatic condition $J = J(\Psi)$, so it must be inherent to both force-free and magnetostatic fields having the axial symmetry. The analogous fact has been early established by Lewis (1990) for toroidal geometry but we derived it in a much simpler way by using a different Hamiltonian and canonical variables.

This structure provides a powerful tool for investigating the geometry of magnetic field lines in our model. Each field line can be considered now as a trajectory in the extended phase space (x, ϖ, θ) of the autonomous one-dimensional dynamical system (27), (28). In the following it turns out that the most interesting behavior of the field lines is outside of the flux tube, where the magnetic field is purely potential and $J(\Psi) \equiv I_0$, so that

$$B_\theta = \frac{\mu_0 I_0}{2\pi r_\perp}. \quad (31)$$

The Hamiltonian (30) then reduces to

$$H = \frac{2\pi \Psi}{\mu_0 I_0 L}, \quad (32)$$

which is simply the poloidal flux function multiplied by a constant. This function is the following linear superposition:

$$\Psi = \Psi_q + \Psi_{-q} + \Psi_I, \quad (33)$$

where the flux functions $\Psi_{\pm q}$ and Ψ_I , respectively, correspond to the charges $\pm q$ and flux tube. The x -component of the field produced by one charge is

$$B_{\pm qx} = \frac{\pm q(x \mp 1)}{[r_{\perp}^2 + (x \mp 1)^2]^{3/2}}, \quad (34)$$

which together with (23) enables us to obtain

$$\Psi_{\pm q} = \frac{\mp q(x \mp 1)}{\sqrt{r_{\perp}^2 + (x \mp 1)^2}}. \quad (35)$$

Let the minor radius a of the flux tube be much less than its major radius R , then Ψ_I must be well approximated outside the tube by the flux function of the circle coil of radius R with current I . Due to the axial symmetry $\Psi_I(r_{\perp}, x) = r_{\perp} A_I(r_{\perp}, x)$, where A_I is one non-vanishing θ -component of the vector-potential

$$\mathbf{A}_I(\mathbf{r}) = \frac{\mu_0 I}{4\pi} \oint \frac{d\mathbf{r}'}{|\mathbf{r} - \mathbf{r}'|},$$

in which the integration is made over the whole coil. After some transformations it gives

$$\Psi_I = \frac{\mu_0 I}{\sqrt{8}} (LRr_{\perp} v)^{1/2} \Phi(v), \quad (36)$$

where

$$v = \frac{2R/L r_{\perp}}{R^2/L^2 + r_{\perp}^2 + x^2}, \quad (37)$$

$$\Phi(v) = \frac{1}{\pi} \int_0^{\pi} \frac{\cos \theta d\theta}{(1 - v \cos \theta)^{1/2}}. \quad (38)$$

One can verify that $\Phi(v)$ is approximated by

$$\Phi(v) \approx 0.043 v - 0.089 v^2 - 0.207 \ln(1 - v) \quad (39)$$

with the relative error $\leq 1\%$ on the interval $[0, 0.9]$, which is good enough for our further purposes.

The Lorenz force $F_q = -2qLI(R^2 + L^2)^{-3/2}$ caused by the interaction of the current I with the fields $B_{\pm qx}$ and the self-force $F_I = \mu_0 I^2 (\ln 8R/a - 5/4)/(4\pi R)$ of the flux tube due to its curvature counterbalance one another if the current is

$$I = \frac{8\pi qLR(R^2 + L^2)^{-3/2}}{\mu_0 [\ln(8R/a) - 5/4]}. \quad (40)$$

The expression for F_I used here corresponds to the simplest case when the equilibrium current I in the tube is uniformly distributed over its circular cross-section of radius a . Other possible current distributions just slightly modify the constant $5/4$ (see Titov & Démoulin 1999). For the assumed small radius of the flux tube ($a \ll R$) the toroidal field B_{θ} is approximately homogeneous in the vicinity of the tube.

This enables us to relate the radius a to the total number n_t of field line turns in the tube as follows:

$$n_t \approx \frac{\mu_0 IR}{2\pi a^2 |B_{\theta}|} = \frac{IR^2}{|I_0| a^2}. \quad (41)$$

In the above mentioned scenario of the emerging flux tube only the equilibrium current I and minor radius a change with growing major radius R according to (40) and (41), while n_t and the other parameters of the model q , d , L , and I_0 remain constant. At each moment of such an evolution Eqs. (32), (33), (35), and (36)–(41) describe the Hamiltonian dynamic system (27)–(28) corresponding to the magnetic field outside the flux tube.

The Hamiltonian in this region has a hyperbolic critical point, which is in fact the X-point of the poloidal magnetic field. Figure 3 shows the corresponding phase portrait of the system for the following set of parameters: $n_t = 5$, $q = 100 \text{ T} \cdot \text{Mm}^2$, $L = 50 \text{ Mm}$, $R = 110 \text{ Mm}$, $I_0 = -7 \text{ TA}$ (cf. Titov & Démoulin 1999b). This portrait is a result of projection $(x, \varpi, \theta) \rightarrow (x, \varpi)$ of several magnetic field lines. It can also be considered as a set of contours $H = \text{const}$, since our autonomous phase flow conserves the Hamiltonian. Taking into account Eq. (32) or more general Eq. (30), one can obtain another useful interpretation of the portrait, namely, as a cross-section $\theta = \text{const}$ of the corresponding poloidal magnetic surfaces $\Psi = \text{const}$ shown in the coordinates (x, ϖ) . These coordinates differ from Cartesian ones only by the logarithmic transformation ($\varpi = \ln r_{\perp}$) of the vertical axis, so Figure 3 yields a rather realistic information about the shape of these surfaces.

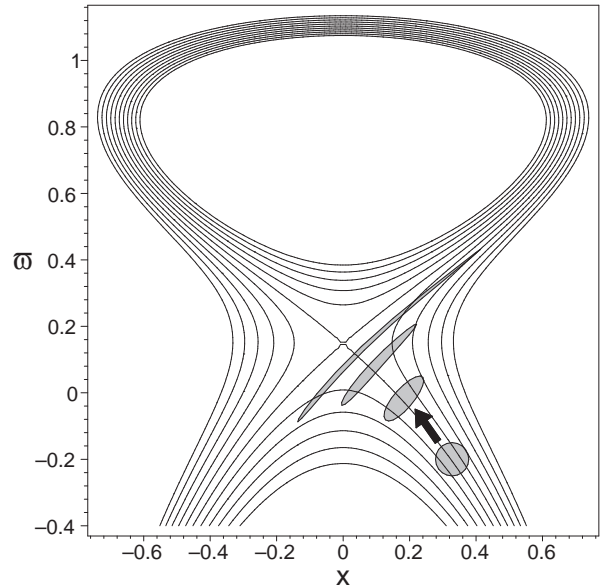


Figure 3. The phase volume at four different equidistant moments: the initial volume is represented by a small circular, which can be considered as the corresponding photospheric cross-section of the flux tube starting near the center of the configuration; the final highly stretched volume corresponds to the moment when the field line, passing through the X-point of the poloidal field, reaches the photosphere.

The important property of autonomous Hamiltonian systems is the conservation of the corresponding phase volume in the phase flow. In our case this volume is two-dimensional, so the area of the plane (x, ϖ) is conserved in such a flow. This property in combination with the presence of the hyperbolic critical point, provides a mechanism of the QSL formation in our configuration. Indeed, any cross-section of an elementary flux tube corresponds to an area in the phase plane and the variation of this cross-section along such a tube corresponds to an evolution of the appropriate phase area due to the phase flow. Given a small circle near one of the separatrices on the phase portrait as an initial area, its area-conserving evolution with the divergent character of the phase flow near the critical point will inevitably cause a stretching and compressing of this area across and along, respectively, the direction of the flow (see Figure 3). This means that the elementary flux tubes starting nearby the poloidal separatrix surfaces have to experience especially strong flattening, which is a characteristic feature of the field lines in QSL.

One can also expect from the above consideration that the maximal value of $Q \equiv Q_X$ is achieved at the field line passing through the X-point of poloidal magnetic field. It is possible to derive an analytical expression for Q_X by first linearizing Eqs. (27)–(28) at the hyperbolic critical point of H and then solving them in order to calculate the corresponding derivatives for Q_X . The final result reads

$$Q_X = 2 + \left(4 + \frac{d^4 L^{-2} r_X^{-2}}{L^2 r_X^2 - d^2} \right) \sinh^2(\lambda \Delta\theta), \quad (42)$$

where r_X ($< R/L$) stands for the dimensionless radius r_\perp corresponding to the X-point of the poloidal field. The value λ is given by

$$\lambda = r_X \left. \frac{\partial^2 H}{\partial x^2} \right|_{x=0, \varpi=\ln r_X} \quad (43)$$

and according to (22), (31) and (32) it characterizes the strength of the poloidal field on the distances $\sim Lr_X$ in comparison with the toroidal field at the X-point. The value

$$\Delta\theta = \pi - 2 \arcsin \left(\frac{d}{Lr_X} \right) \quad (44)$$

determines the arc length of the coronal part of the field line passing through the X-point.

Eq. (42) shows that Q_X grows exponentially with $\lambda \Delta\theta$, so Q_X strongly depends on the relationship between poloidal and toroidal components in the vicinity of the X-point and the length of the field line passing through this point. This value has been computed for the above mentioned parameters and $d = 50$ Mm in the scenario of the emerging flux tube. The dependence $Q_X(R)$ at several different values of I_0 (see Figure (4)) suggests that the QSL has to appear in the twisted configuration when the major radius of the flux tube reaches $R \gtrsim 100$ Mm. This corresponds approximately to the moment when the genuine separatrix surfaces (caused by BPs) disappear (Titov & Démoulin 1999b).

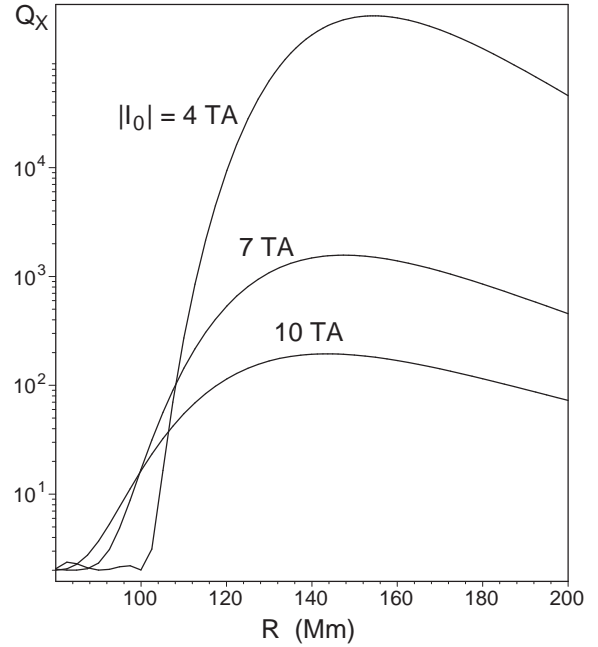


Figure 4. The dependence of $Q \equiv Q_X$ on the radius of the flux tube R for the field line passing through the X-point of poloidal magnetic field at different values of the line current I_0 (Figure 2).

5. CONCLUSIONS

In this paper, new results concerning the theory of the quasi-separatrix layers (QSLs) in coronal magnetic fields are reported. We have revised the previous definition of QSLs (Priest & Démoulin 1995) by analyzing the local geometrical properties of the field line connectivity. This analysis provides a new geometrical measure Q , which determines the degree of flattening of the elementary flux tubes. Contrary to the so-called norm N proposed previously by Priest & Démoulin (1995), the new measure Q yields the same results for both positive and negative magnetic polarities on the photosphere. In other words, Q characterizes the magnetic connectivity itself rather than the corresponding field line mappings (from positive to negative polarity or vice versa).

The old and new measures are related by a very simple formula $Q = N^2/\Delta$, in which Δ is the Jacobian of the corresponding field line mapping. Thus, if Δ varies on the photosphere as strong as N , the new and old measure must yield different locations for QSLs.

We have applied this theory to the model of twisted magnetic configuration proposed in (Titov & Démoulin 1999ab) for the analysis of magnetic topology in sigmoid-like solar flares. It has been demonstrated that the appearance of QSLs in such a model is related with the Hamiltonian structure of the modeling magnetic field: the conservation of the phase area in the corresponding phase flow and the presence of the X-point in the poloidal magnetic field provides the mechanism for the formation of QSLs in this configuration. The results of computations of Q suggest that the QSL must be formed in such

a configuration approximately after that the genuine separatrix surfaces disappear when the twisted flux tube emerges high enough into the corona.

ACKNOWLEDGMENTS

V.S. Titov and G. Hornig gratefully acknowledge financial support from Volkswagen-Foundation.

REFERENCES

- Démoulin, P., Hénoux, J.C. , Mandrini C.H. 1994, A&A 285, 1023
- Démoulin, P., Bagalá, L.G., Mandrini, C.H. et al. 1997, A&A 325, 305
- Inverarity, G. W., Titov, V. S. 1997, JGR 102, 22285
- Lau, Y.-T. 1993, Solar Phys. 148, 301
- Lewis, H. R. 1990, Phys. Fluids B 2, 2551
- Low, B.C., Wolfson, R. 1988, ApJ 324, 574
- Mandrini, C.H., Démoulin, P., Rovira, M.G. et al. 1995, A&A 303, 927
- Priest, E.R. , Démoulin, P. 1995, JGR 100, A12, 23443
- Schindler, K., Birn, J., 1999, JGR in press
- Seehafer, N. 1986, Solar Phys. 105, 223
- Titov, V.S. , Priest, E.R., Démoulin, P. 1993, A&A 276, 564
- Titov, V.S. , Démoulin, P. 1999, PASP conf. ser. 184, 76
- Titov, V.S. , Démoulin, P. 1999, A&A in press
- Vekstein, G.E., Priest E.R., Amari, T. 1991, A&A 243, 492
- Vekstein, G.E., Priest, E.R. 1992, ApJ 384, 333
- Zwingmann, W., Schindler K., Birn, J. 1985, Solar Phys. 99, 133